Artificial Bio-inspired Tactile Receptive Fields for Edge Orientation Classification

Ali Dabbous[1,2], *Member*, *IEEE*, Michele Mastella[3,4], *Student Member*, *IEEE*, Aishwarya Natarajan[5], Elisabetta Chicca.[3,4], *Senior Member*, *IEEE*, Maurizio Valle[1], *Senior Member*, *IEEE*, Chiara Bartolozzi[2], *Member*, *IEEE*

***Abstract*—Robots and users of hand prosthesis could easily manipulate objects if endowed with the sense of touch. Towards this goal, information about touched objects and surfaces has to be inferred from raw data coming from the sensors. An important cue for objects discrimination is the orientation of edges, that is used both in artificial vision and touch as pre-processing stage. We present a spiking neural network, inspired on the encoding of edges in human first order tactile afferents. The network uses three layers of Leaky Integrate and Fire neurons to distinguish different edge orientations of a bar pressed on the artificial skin of the iCub robot. The architecture is successfully able to discriminate eight different orientations (from 0^o to 180^o), by implementing a structured model of overlapping receptive fields. We demonstrate that the network can learn the appropriate connectivity through unsupervised spike based learning, and that the number and spatial distribution of sensitive areas within the receptive fields are important in edge orientation discrimination.**

***Index Terms*—Touch, Skin, Receptive Fields, SDSP, Neuromorphic**

I. Introduction

The sense of touch is an important gateway to interact with the environment [1]. Robots and hand prosthesis endowed with the sense of touch can better and more easily manipulate objects, and physically collaborate with other agents. Different types of biologically inspired sensors have been developed based on various transduction techniques (e.g. capacitive, piezoresistive, optical, magnetic, binary and piezoelectric). Most of them sample the transducer at a fixed time, generating a huge amount of data, even when the device is not in contact with a stimulus, and introducing a latency that can be critical in dangerous situations, when a fast reaction time is needed as escape reflex from dangerous contacts. On the other hand, biological sensors react to changes in the sensory signal, rather than sampling the sensory signal at fixed time intervals. This characteristic is known as event or data driven sensing. As it conveys data only at change, it reduces redundancy (no samples for constant signal), while it increases the sampling rate for fast changes. While neuromorphic circuits are being developed to encode the continuous analog signal from physical transducers into spikes [2], [3], sigma-delta conversion [4] or spiking neuron models can be used to convert the signals generated by front-end clocked artificial tactile sensors to neuromorphic spikes [1]. At the same time, in both biological and artificial sensory systems, feature extraction is an important stage to extract information from the sensory signals. Edge orientation selective neurons have been observed in the first order tactile afferents of human fingertips [5] [6] [7], and it is often used in artificial vision and touch as pre-processing stage. In [5], recordings of human fingertips responses show that information about edge orientation emerges in neurons responsible for detecting the coincident activation of afferents with overlapping and interleaved receptive fields. In [8] to discriminate between different edge orientation at any location on simulated mechanoreceptor skin patch, they proposed 3 layers spiking neural model starting with first-order neurons to encode input stimulus into spike trains and ending with cortical neurons to decode edge orientation. In robots, several solutions have been employed for fine orientation detection (up to 5^o) on artificial skin, ranging from an AI-based vector regression method with offline learning [9] to a more neuromorphic approach with spike-based classification and differential delay lines, inspired on the cuneate nucleus neurons [10]. Those solutions, due to the need for offline learning and the presence of structures not easily transferable in silicon, lack the possibility to be embedded on robots or prosthetic devices. In such cases, where space and energy are constraints, a hardware implementation with online learning and low power devices is usually preferred, as it enables the system to perform end-to-end computation from the sensors to the processing and classification, consuming low power. We therefore targeted the development of an edge orientation architecture based on event-driven acquisition and unsupervised spike-driven learning that can be implemented on low-power neuromorphic hardware. We present a neuromorphic model for edge orientation selectivity inspired by the finding of [5], based

A.D. and M.V acknowledge partial financial support from Tactile feedback enriched virtual interaction through virtual reality and beyond (TACTILITY) project: EU H2020, Topic ICT-25-2018-2020, RIA, Proposal ID 856718. M.M., C.B. and E.C acknowledge partial financial support from EU H2020 project Neutouch grant No. 813713. M.M. and E.C would like to acknowledge the financial support of the CogniGron research center and the Ubbo Emmius Funds (Univ. of Groningen).

Affiliation:
[1] Connected Objects Sensing Materials Integrated Circuits (COSMIC) lab. University of Genova-DITEN, Genova, Italy.
[2] Event-Driven Perception for Robotics (EDPR) lab. Istituto Italiano Di Tecnologia (IIT), Genova, Italy.
[3] Bio-Inspired Circuits and Systems (BICS) Lab. Zernike Institute for Advanced Materials (Zernike Inst Adv Mat), University of Groningen (Univ Groningen), Nijenborgh 4, NL-9747 AG Groningen, Netherlands.
[4] CogniGron (Groningen Cognitive Systems and Materials Center), University of Groningen (Univ Groningen), Nijenborgh 4, NL-9747 AG Groningen, Netherlands.
[5] Georgia Institute of Technology, Atlanta, Georgia, United States

on computational primitives that are implementable on low-power subthreshold neuromorphic hardware, going towards the design of artificial skin with pre-processing embedded capabilities. We used, as front-end sensors, the capacitive skin of the iCub robot [11]. The acquired pressure values are encoded into spike trains by means of Leaky Integrate and Fire (LIF) neurons. An additional layer of neurons, representing afferent fibers, collects the stimuli coming from the encoding neurons using overlapping and interleaved receptive fields. The last layer detects coincident activity of subsets of neurons in the previous layer, to decode the stimulus orientation. We characterized the network to reproduce the orientation selectivity observed by [5] (Sec. III-A). We then endowed the network with a local unsupervised learning rule between the afferent and decoding layers (Sec. III-B). As learning rule, we implemented a biologically plausible model that exploits the temporal correlation of input spikes and neuron's activity. Finally, we explored different topologies of the interleaved receptive fields, defining how the single sensitive areas (taxels) are distributed in the receptive fields (Sec. IV). The model is able to discriminate between eight different orientations (0^o to 180^o with 22.5^o increments), and it can learn an appropriate connectivity pattern for the classification. Finally, the receptive fields created by randomly selecting sensitive points perform better than structured receptive fields with uniform distribution in discriminating small angles (down to 5^o).

II. Network Architecture

In [5] the neural architecture that gives rise to edge orientation selectivity is based on a network composed of two layers. The first layer consists of neurons with overlapping receptive fields, where each neuron possesses a distinct distribution of highly sensitive zones on the skin. At a given moment, a given edge activates simultaneously a subset of neurons. The second layer is able to spot the temporal coincident activation between these neurons and decode the input stimulus orientation.

We developed a spiking neural network based on such a model, consisting of a patch of artificial skin from the iCub robot [11] and three layers of LIF neurons [12], as shown in Fig. 1, where resting membrane potential v_{rest} is -70mV, membrane capacitance C_m is 0.25 nF, membrane threshold V_{th} is -50mV, and refractory period is 2ms. The skin patch (11 cm x 7.5 cm) comprises 160 capacitive tactile sensing elements (taxels) distributed along 16 triangles (10 taxels each). The variation in capacitance is detected by the taxels through the interaction between a copper plate and a human fingertip or other conductive materials [13]. Layer one represents the encoding layer and consists of 24 LIF neurons. The patch of skin and layer one neurons model the output of biological mechanoreceptors. Every neuron in layer one is connected to a single taxel in the skin patch. The output pressure of the taxels is used as input to LIF neurons in layer one for encoding analog data into spikes (Figure 1-A). Layer two consists of 5 neurons that represent the overlapping receptive fields that receive input spikes from the input mechanoreceptors layer (Figure 1-B). The third (and last) layer consists of 8 LIF

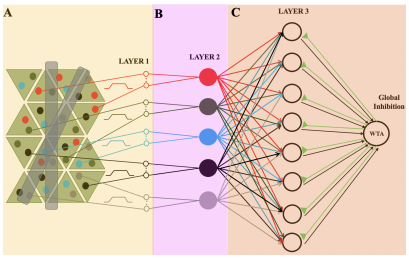

Fig. 1. Spiking neural network for edge orientation: (A) Skin patch from the iCub robot and layer one, which encodes the analog signal into spikes. (B) First order tactile neurons (layer two) gathering the 160 inputs from layer one, organised in receptive fields. (C) Layer three discriminates edge orientation and includes a global inhibitory neuron that implements the WTA network.

neurons (one neuron per orientation) that decode different orientations using the temporal coincidence activation of layer two. We designed a structure of overlapping receptive fields such that, for every orientation, three neurons would be activated simultaneously. The connectivity between layer two and layer three was hard-wired to ensure the activation of a specific neuron from last layer for the each orientation. For better selectivity, layer three employs a Winner-Take-All (WTA) structure, composed by a global inhibitory neuron that receives excitation from all neurons (black synapses in Figure 1-C) and in turn inhibits the activity of all of them, so that only the neuron receiving the highest input can be active (green synapses in Figure 1-C). The data was collected by pressing a bar (13cm x 9mm) on the skin in different orientations. During the contact, the analog pressure measured by each capacitor sensor (taxel) was recorded using a setup comprising a ZynQ7000 board connected to the skin patch and the Yet Another Robot Platform (YARP) middle-ware [14]. The recorded pressure signal was injected as input current into the LIF neurons in layer one (Figure 1-A), simulated with Brian2 [15].

III. Learning Orientations with Designed Receptive Fields

A. Fixed Connectivity

To test the ability of our model architecture in discriminating different edge orientations that are applied on the skin, we fixed the connectivity between layer two and layer three in the network architecture, (Figure 1-C). Based on the receptive field structure described in the previous section, we chose three active sensors for every orientation where these sensors are connected one to one connection with three neurons in layer one and then connected the three neurons manually to three different receptive fields in layer two. For each orientation, only three neurons in layer two were activated at the same time. The combination of the activated neurons in layer two at each orientation was connected to a single neuron in layer three. The coincident spiking activity of the three neurons of layer two increases the membrane potential of the neuron in layer three, causing it to spike. As a result, each neuron in the third layer is selective to a given orientation, increasing its firing rate for orientations close to its preferred orientation and showing maximum firing rate in response

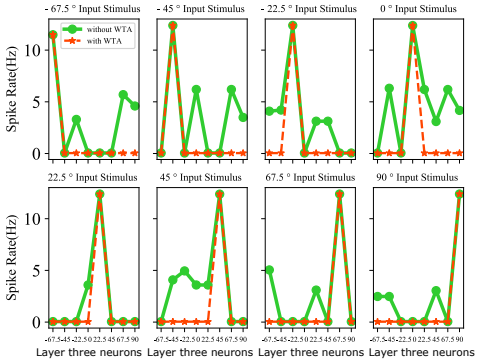

Fig. 2. Firing rates of neurons in layer three for different stimulus orientations (fixed connectivity); with (red) and without (green) WTA.

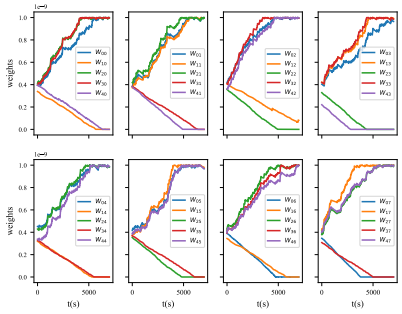

Fig. 3. Variation of the synaptic weight for each presynaptic spike as a function of time. Each box represents the synaptic weights between j_{th} neurons in layer two and i_{th} neuron in layer three.

to the one for which it is tuned. For each of the different orientations, there is only one neuron from layer three that has a maximum firing rate. Some neurons fire several spikes also for orientations that do not have their exact combination of receptive fields, but a similar one. To increase orientation selectivity, we implemented WTA competition, using a global inhibitory neuron [16]. Fig. 2 shows the comparison of the mean firing rate of each neuron in layer three with and without the WTA (orange and green lines respectively). The network was able to detect eight different peaks through applying eight distinct input stimuli each having a different orientation. This confirms that the model can discriminate between several distinct edge orientations applied on artificial skin.

B. Unsupervised Learning of Edge Orientation

We aimed to examine whether the system can build the right connectivity through local unsupervised learning and to find the optimal structure for orientation selectivity. To achieve that aim, we endowed the network with a local unsupervised synaptic learning rule Spike Driven Synaptic Plasticity (SDSP) [17] between layer two and layer three with all to all connection as shown in Figure 1-C. Our goal was to make the network learn the different orientations using temporal coincidence. SDSP can be achieved using a combination of depolarization and an effective neuronal model of the postsynaptic layer (layer three), where the current supplied from layer two is defined as

$$I_{ex}(t) = \sum_{i=1}^{n} \left(w_{2_{ji}} \sum_{k} S_{1_i}(t - t_k) \right) \tag{1}$$

S_{1_i} represents the spatio-temporal input spikes of the i_{th} neuron. t_k is the time in which the neurons in layer two fire a spike. The change of SDSP synaptic dynamic w_2 between the j_{th} neuron in layer two and the i_{th} neuron in layer three depends on the depolarization of the postsynaptic membrane potential and the slow postsynaptic calcium variable, C(t) defined as

$$\frac{dC}{dt} = \frac{C}{\tau_C} + J_C \sum_{i} \delta(t - t_i) \tag{2}$$

In this equation, the sum represents the postsynaptic spike, arriving at times t_i. J_c is the spike's current contribution and τ_C is the calcium time constant.

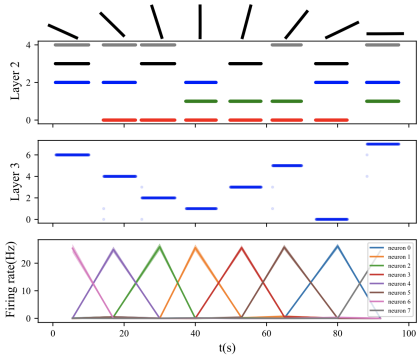

Fig. 4. SDSP learning rule; (top) Output spikes of layer two: each orientation corresponds to the activation of three neurons; (middle) Output spikes of neurons in layer three: only one neuron is firing for each orientation; (bottom) Mean firing rate and standard deviation (shadow) of each neuron for each orientation.

During the learning phase, the output layer is fed with multiple stimulus presentations in series, randomly repeating the eight different orientations, 35 times each. Each stimulus presentation is encoded in the spiking activity of three neurons of the second layer. When a third layer neuron spikes then the synaptic weights connecting this neuron and the three active neurons from layer two are increased. The remaining two connections are instead depressed. The synaptic weights between the two layers were initialized using uniform random distribution. During learning, synaptic weights progressively change, converging to a stable connectivity pattern, as shown in Figure 3. After learning, the network is able to discriminate 8 different orientations applied to the skin, from 0^o to 180^o in 22.5^o increments. To validate our system, we extracted the learned weights and tested the network by applying different datasets, each with the 8 different orientations. Figure 4 shows the raster plots of layer two for the 8 different orientations, along with the raster plot of layer three after decoding the orientation. For every pattern, only one neuron in layer three is firing at maximum firing rate and only for a specific orientation (bottom box in Figure 4).

IV. Receptive Field Structure

In section III we analyzed the response of the model to a manually designed set of receptive fields inspired by the

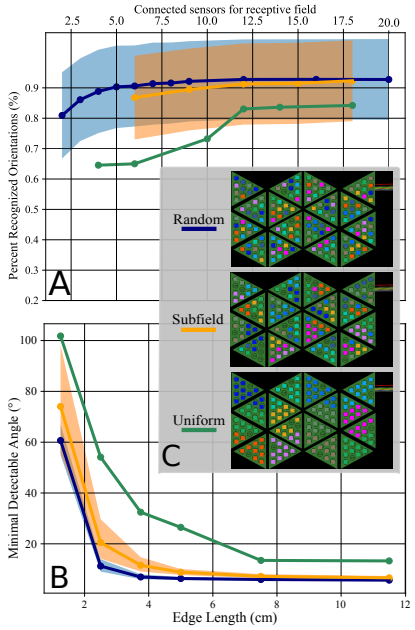

Fig. 5. Receptive fields' topologies: A) Fraction of recognised orientations for each receptive fields' structure, as a function of connected sensing elements (mean and std shaded). B) Minimum detectable angle as a function of bar length (mean and std shaded). C) One example for each of the three topologies.

finding of [5]. Here we verify the hypothesis that receptive fields with random (and interleaved) sensitive points can offer higher orientation acuity than receptive fields where sensitive points are positioned uniformly [6]. Following this approach, we investigated different receptive fields topologies with three different connectivity patterns shown in Fig. 5C:

- Uniform: the skin is divided in different and homogeneous receptive fields grouping the sensitive elements into regions.
- Random: the sensitive elements on the whole skin are randomly associated to different receptive fields.
- Random with subfields: the receptive field is composed of small clusters of adjacent sensing elements, randomly placed on the skin (different from the random structure where each taxel is independent of its neighbors).

The activity of the receptive fields' layer encodes the orientation of the bar through a spatial code defined at each temporal window (the time during which a stimulus is presented). In said time, the neurons that have a spike activity higher than an arbitrary threshold (defined as half the spike rate of the most active neuron) are considered as '1' while the other ones as '0'. To assess the quality of the neural code generated by said layer we used mutual information. For each trial we counted the times a given spatial code appeared in relation to a bar's orientation. This results in a joint probability table of size $R \times S$, where R represents the spatial code responses and S the stimulus orientation. Using mutual information (MI) [18], we computed how much information about the input orientation the system can encode. We firstly recreated the experiment where a bar is pressed on the skin at eight different orientations, but changing the configuration of the receptive fields according to the three proposed topologies. This was repeated multiple times, while decreasing the number of taxels impinging to each receptive field. Fig. 5A shows the fraction of recognised orientations (calculated as $2^{MI}/8$) computed for every different topology and for the number of taxels per receptive field. The taxels' number variation is meant to estimate the robustness of each topology to edge orientation encoding when the receptive fields density decreases. We then simulated a bar applied on the skin with different lengths and orientations. The way the taxels were distributed followed again the three different topologies. We measured the minimum angle detectable by the network dividing the maximum angle excursion and the number of detected orientations ($Angle(^\circ) = \frac{Maximum\ excursion}{Number\ of\ orientations} = \frac{180^\circ}{2^{MI}}$).

We then simulated an increased number of bar's orientations in order to calculate the minimum angle that the different topologies could discriminate, and changed the length of the bar to estimate robustness to the decreasing level of information about the stimulus, due to the shortening of the bar. We applied 36 different angles (180° with 5° steps) with the length of the bar changing from 1cm to 11cm with a 1cm step. Each configuration was repeated for 150 trials. The results, visible in Figure 5B, highlight that, given a fixed length, the receptive fields with fully random distribution seem to perform better in orientation acuity. As expected, the orientation discrimination, gracefully degrades with decreasing stimulus length.

V. Conclusion

We developed a biologically inspired spiking network composed of three layers of LIF neurons to discriminate different edge orientations of a bar pressed on artificial skin. The network is capable of discriminating between eight different orientations by adopting a model of overlapping and interleaved receptive fields that exploits temporal coincidence of the activation of neurons with different receptive fields. Thanks to the encoding, based on temporal coincidence, the network also has the ability to build up the required connectivity, when endowed with spike-based unsupervised learning. Finally, through following biological examples [6] in which sensitive areas of the receptive fields are randomly distributed on the skin, we proposed an approach for estimating the optimal distribution of taxels in receptive fields for increasing the orientation acuity. This method can be used as a tool to minimise the connectivity and number of required taxels in future generations of artificial skin, while maintaining spatial sensitivity. This preliminary work calls for further studies on biologically inspired orientation selectivity and feature extraction for artificial skin. The development shall exploit temporal coincidence, also exploring the role of different types of receptors and spiking encoding. Specifically, we will keep on resorting to computational primitives that have a correspondent hardware implementation using neuromorphic sub-threshold CMOS technology, and we will integrate neuromorphic event-driven readout of the analog values measured by the physical pressure transducers, with the aim of designing compact and efficient sensing devices that can locally pre-process the tactile signal.

REFERENCES

[1] Z. Yi, Y. Zhang, and J. Peters, "Biomimetic tactile sensors and signal processing with spike trains: A review," *Sensors and Actuators A: Physical*, vol. 269, pp. 41–52, 2018.

[2] S. Caviglia, L. Pinna, M. Valle, and C. Bartolozzi, "Spike-based readout of posfet tactile sensors," *IEEE Transactions on Circuits and Systems I: Regular Papers*, vol. 64, no. 6, pp. 1421–1431, 2016.

[3] M. Rasouli, Y. Chen, A. Basu, S. L. Kukreja, and N. V. Thakor, "An extreme learning machine-based neuromorphic tactile sensing system for texture recognition," *IEEE transactions on biomedical circuits and systems*, vol. 12, no. 2, pp. 313–325, 2018.

[4] C. Bartolozzi, P. M. Ros, F. Diotalevi, N. Jamali, L. Natale, M. Crepaldi, and D. Demarchi, "Event-driven encoding of off-the-shelf tactile sensors for compression and latency optimisation for robotic skin," in *2017 IEEE/RSJ International Conference on Intelligent Robots and Systems (IROS)*. IEEE, 2017, pp. 166–173.

[5] J. A. Pruszynski and R. S. Johansson, "Edge-orientation processing in first-order tactile neurons," *Nature neuroscience*, vol. 17, no. 10, pp. 1404–1409, 2014.

[6] J. A. Pruszynski, J. R. Flanagan, and R. S. Johansson, "Fast and accurate edge orientation processing during object manipulation," *Elife*, vol. 7, p. e31200, 2018.

[7] B. P. Delhaye, X. Xia, and S. J. Bensmaia, "Rapid geometric feature signaling in the simulated spiking activity of a complete population of tactile nerve fibers," *Journal of neurophysiology*, vol. 121, no. 6, pp. 2071–2082, 2019.

[8] A. Parvizi-Fard, M. Amiri, D. Kumar, M. M. Iskarous, and N. V. Thakor, "A functional spiking neuronal network for tactile sensing pathway to process edge orientation," *Scientific reports*, vol. 11, no. 1, pp. 1–16, 2021.

[9] R. D. P. Wong, R. B. Hellman, and V. J. Santos, "Spatial asymmetry in tactile sensor skin deformation aids perception of edge orientation during haptic exploration," *IEEE Transactions on Haptics*, vol. 7, no. 2, pp. 191–202, 2013.

[10] U. B. Rongala, A. Mazzoni, M. Chiurazzi, D. Camboni, M. Milazzo, L. Massari, G. Ciuti, S. Roccella, P. Dario, and C. M. Oddo, "Tactile decoding of edge orientation with artificial cuneate neurons in dynamic conditions," *Frontiers in neurorobotics*, vol. 13, p. 44, 2019.

[11] G. Metta, L. Natale, F. Nori, G. Sandini, D. Vernon, L. Fadiga, C. Von Hofsten, K. Rosander, M. Lopes, J. Santos-Victor *et al.*, "The icub humanoid robot: An open-systems platform for research in cognitive development," *Neural networks*, vol. 23, no. 8-9, pp. 1125–1134, 2010.

[12] P. U. Diehl and M. Cook, "Unsupervised learning of digit recognition using spike-timing-dependent plasticity," *Frontiers in computational neuroscience*, vol. 9, p. 99, 2015.

[13] G. Cannata, M. Maggiali, G. Metta, and G. Sandini, "An embedded artificial skin for humanoid robots," in *2008 IEEE International conference on multisensor fusion and integration for intelligent systems*. IEEE, 2008, pp. 434–438.

[14] L. Natale, A. Paikan, M. Randazzo, and D. E. Domenichelli, "The icub software architecture: Evolution and lessons learned," *Frontiers in Robotics and AI*, vol. 3, p. 24, 2016.

[15] M. Stimberg, R. Brette, and D. F. Goodman, "Brian 2, an intuitive and efficient neural simulator," *eLife*, vol. 8, p. e47314, Aug. 2019.

[16] E. Chicca, G. Indiveri, and R. J. Douglas, "An event-based vlsi network of integrate-and-fire neurons," in *2004 IEEE International Symposium on Circuits and Systems (ISCAS)*, vol. 5. IEEE, 2004, pp. V–357.

[17] J. M. Brader, W. Senn, and S. Fusi, "Learning real-world stimuli in a neural network with spike-driven synaptic dynamics," *Neural computation*, vol. 19, no. 11, pp. 2881–2912, 2007.

[18] N. M. Timme and C. Lapish, "A Tutorial for Information Theory in Neuroscience," *eneuro*, vol. 5, no. 3, May 2018.